Tuning Process Parameters for Multi-Material Extrusion Through In-house Nozzle System for 3D Bio-printing Process Abstract ID: 2584

Connor Quigley, Warren Hurd, Scott Clark, Rokeya Sarah, and MD Ahasan Habib*

Sustainable Product Design and Architecture Department, Keene State College, Keene, NH 03435, USA.

Abstract

The emerging field of three-dimensional bio-printing seeks to recreate functional tissues for medical and pharmaceutical purposes. With the ability to print diverse materials containing different living cells, this growing area may bring us closer to achieving tissue regeneration. In previous research, we developed a Y-shaped nozzle connection device that facilitated the continuous deposition of materials across multiple filaments. This plastic device had a fixed switching angle and was intended for single use. In this study, we present an extension of our previous nozzle system. To fabricate the nozzle connectors, we chose stainless steel and considered angles of 30°, 45°, and 90° (both vertical and tilted) between the two materials. The total material switching time was recorded and compared to analyze the effects of these angles. We used our previously developed hybrid hydrogel (4% Alginate and 4% Carboxymethyl Cellulose, CMC) as a test material to flow through the nozzle system. These in-house fabricated nozzle connectors are reusable, and sterile and enable smooth material transition and flow.

Keywords

3D bioprinting, Rheology, Shear Thinning, Printability.

1. Introduction

The use of various biomaterials encasing living cells in three dimensions (3D) is widely acknowledged for the fabrication of patient-specific complicated models [2]. As a developing tool for tissue engineering, this method is crawling toward closely mimicking tissue-specific microarchitecture. Extrusion-based 3D bioprinting method allows for better deposit of a variety of biomaterials with a higher percentage of cells encapsulated compared to laser and ink jet bioprinting [3]. Due to their biocompatibility, low cytotoxicity, and high water content (90%), natural hydrogels make excellent options for bio-ink (biomaterial encapsulating living cells) [4]. However, due to their poor mechanical strength and slow crosslinking rate, only a small number of them are normally employed to prepare bio-ink [5]. Successful cell-to-cell communication can speed up the regeneration of damaged tissue [6]. Consequently, the ability to create scaffolds from a variety of materials that include various type of cells can mimic the native tissue architecture and take the tissue regeneration effort one step further [7]. There have been several reported attempts to construct scaffolds out of different materials. It has been reported to manufacture polycaprolactone (PCL) and alginate scaffolds using chondrocyte and osteoblast cells using a multi-head bioprinting approach [8]. An effort was described using altering chemical, electrical, mechanical, and biological properties by modifying process and material associated parameters to demonstrate the capacity to print heterogeneous and multi-functional hydrogel structures [9]. Multihead bioprinters were used to print polyurethane [10] with C2C12 cell and poly(-caprolactone) (PCL) with NIH/3T3 cell in order to combine elasticity and muscle growth on one side and stiffness and tendon development on the other [11]. Multiple print heads have been employed in other works to create multi-material scaffolds, according to reports

Recently, we developed a nozzle system that can switch materials continuously between several filaments [15]. The whole setup was composed of plastic, had a switching angle of 30°, and was designed for single use. The nozzle system we previously suggested is expanded in this study. We took into account angles of 30°, 45°, and 90° (vertical and slanted) between the two materials and decided to construct those nozzle connectors out of stainless steel. To evaluate the effects of those different angles, the total material switching time was recorded and compared. A test substance was employed to see how well our previously created hybrid hydrogel (4% Alginate and 4% Carboxymethyl Cellulose, CMC) [16] flowed through the nozzle system. These locally manufactured nozzle connections are reusable and simple to use.

2. Materials and Methods

2.1 Material flow simulation

SolidWorks 3D Modeling and Flow Simulation Package (Dassault Systèmes SolidWorks Corporation, Waltham, MA) were used to model the nozzle connectors having 30°, 45°, 60°, and 90° angles (vertical and tilted) between the two material flows.

2.2 Transition time calculations and 3D printing

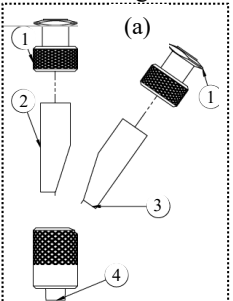
Hydrogels were extruded using a three-axis multi-head (three-extruders) 3D bioprinter (BioX, CELLINK, Boston, MA). In this proposed nozzle system, the material transition time, or the amount of time needed to switch the material flow from one type (100% M1 from vertical) to another type (100% M2 from slanted), was calculated as illustrated in Figure 1. (e). The pressure applied to M₁ was not exerted during the extrusion of M₂. Up until it reached the tip, material from one nozzle was fully extruded into the vacant nozzle connector. Then, the substance from the other nozzle was constantly extruded until it was clearly visible at the nozzle tip. To determine how the angle variation influences the material transition, the time needed for each angle was measured and studied. 4% Alginate and 4% CMC; A₄C₄; our previously created hybrid hydrogel [16] was utilized as a test material to flow through the nozzle system. At least three samples were fabricated each time to confirm the repeatability.

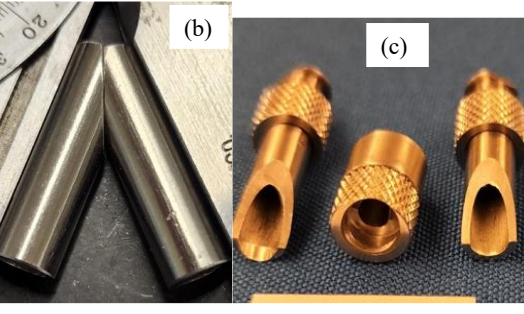
The prepared A_4C_4 hybrid hydrogel was stored in two disposal syringes and extruded pneumatically in a layer-uponlayer way through a 410 μ m (0.41mm) diameter nozzle on a stationary build plane to manufacture the scaffolds extruding through nozzle connectors having 30° , 45° , and 90° angles. The rate at which material is deposited can be affected by a variety of printing parameters, including diameter, air pressure, nozzle speed, and print distance (i.e., the space between the nozzle tip and print bed) [17]. The scaffold was built using a printer with a 10 mm/s print speed and a 0.405 mm print distance.

Rhino 6.0 (https://www.rhino3d.com), a CAD software, was used to create and specify the vectorized toolpath of a scaffold. A Bio-X compliant file containing the toolpath coordinates and all process parameters is created using Slicer (https://www.slicer.org), a G-code generation program, to manufacture the scaffold. A₄C₄ was made and either red or blue food coloring was used to tint the two syringes. Both syringes had check valves placed between the nozzle and syringes, and they were then loaded onto the printer. The printing tip was a 0.41mm plastic tapered syringe tip. Each syringe was pressurized initially to fill in the empty space of the nozzle. They were pressurized until only one material was coming out of the plastic tip. The model used to print was a prismatic box 20mm x 20mm x 1mm, the layer height, infill percentage, print pressure, and print speed were set to 0.3mm, 11%, 110-130kPa, and 7 mm/s respectively. The print was recorded to examine the color-changing and mixing behavior. The overall scaffold fabrication process is schematically shown in Figure 1.

2.3 Fabrication of metallic nozzle

Stainless-steel 303 Leur fittings and Stainless-steel tubing 304 and were acquired from McMaster-Carr McMaster-Carr (Elmhurst, IL). To fit onto the 304 stainless steel tube, the fittings had to be altered on-site using a Bridgeport machine. Our earlier plastic prototype fitting had an Outer Diameter (OD) and Inner Diameter (ID) of 0.250 inch and 0.249 inch, respectively. The ID of the tubing used for four connectors in this paper was 0.169 inch and the OD was 0.249 inch. The tubing was initially cut to 0.8 inch in length using a little horizontal bandsaw (General International: Model BS5205, Whitehouse, OH). On a Bridgeport Milling Machine (Atlanta, GA) equipped with a rapid release C5 collet fixture to hold the tube, the ends were next machined perpendicularly. To adjust various angles, a tool with a three-jaw chuck was put on a different Bridgeport machine. Each component had a pair of tubes. The 90-degree fitment was an exception. For the sake of simpler manufacture, that cut was not done at the end of the tube. A relief cut with a 0.1562-inch diameter cutter was created on one part of the pair to allow clearance for the flow after the cut was made, turning the three-jaw chuck 180° degrees.







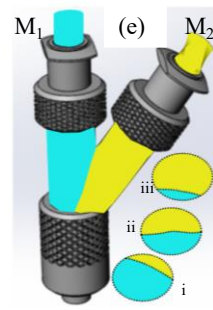


Figure 1: (a) Exploded view of nozzle having 30° connections, (b) Milled parts for 30° , (c) Three parts ready to weld (scale bar 6 mm), (d) Final part (scale bar 28 mm), and (e) An schematic of material distribution with cross-section at three locations, (i) % of M_1 >% of M_2 , (ii) % of M_1 =% of M_2 , (iii) % of M_1 =% of M_2 .

The parts were hand-assembled and a Coherent Rofin StarWelder (Baasel Lasertech, Gilching, Germany) was used to fuse them together. The components were held under a microscope as a foot pedal delivered single laser pulses. Each pulse had a duration of 5 ms, an average power of 2.3 kW, and a diameter of 0.3 mm. Five segments make up the pulse form, each with a power setting of 80%, 100%, 90%, 75%, or 50%. There was between 50% and 75% pulse overlap. Every exterior seam was welded. To fix any gaps, some filler wire made of stainless steel 304 was used. The decreased sulfur level of the 304 stainless in the tubing made it simpler to weld. After being cleaned with a little wire brush, the components were put back into the corresponding baggies. The entire nozzle manufacturing process is shown in Figure 1(b-d).

2.4 Statistical analysis

We collected data following a format of "mean \pm standard deviation" and analyzed them using a significance level of p = 0.05 with a two-way ANOVA. Calculations were done with n=3 unless otherwise stated. We used a statistical software, Origin Pro 2022b (OriginLab, Northampton, MA) to analyze quantitatively and graphically.

3. Results and discussions

3.1 Flow simulations for various nozzle connectors

Flow simulations for 30°, 45°, and 90° nozzles were conducted for three different applied pressures such as 181325, 201325, and 221325 Pa from nozzle tip to the end point of the arrangement. From the shear rate distribution for each nozzle connector, it is clear that higher applied pressure showed larger shear rate at the tip. Figure 2(a) shows shear stress distribution for 201325 Pa applied pressure where a small backflow was observed. None of the designs were able to negate backflow on their own, but the problem was easily fixed by using check valves. Figure 2(b) shows overall shear strain distribution for three applied pressures of 181325, 201325, and 221325 Pa from nozzle tip to 73.47 mm. The simulation result shows 50% and 20% higher shear rate for 22% and 10% increment of applied pressure compared to the applied pressure of 181325 Pa. Similar characteristics were resulted in for 45°, and 90° nozzle connectors.

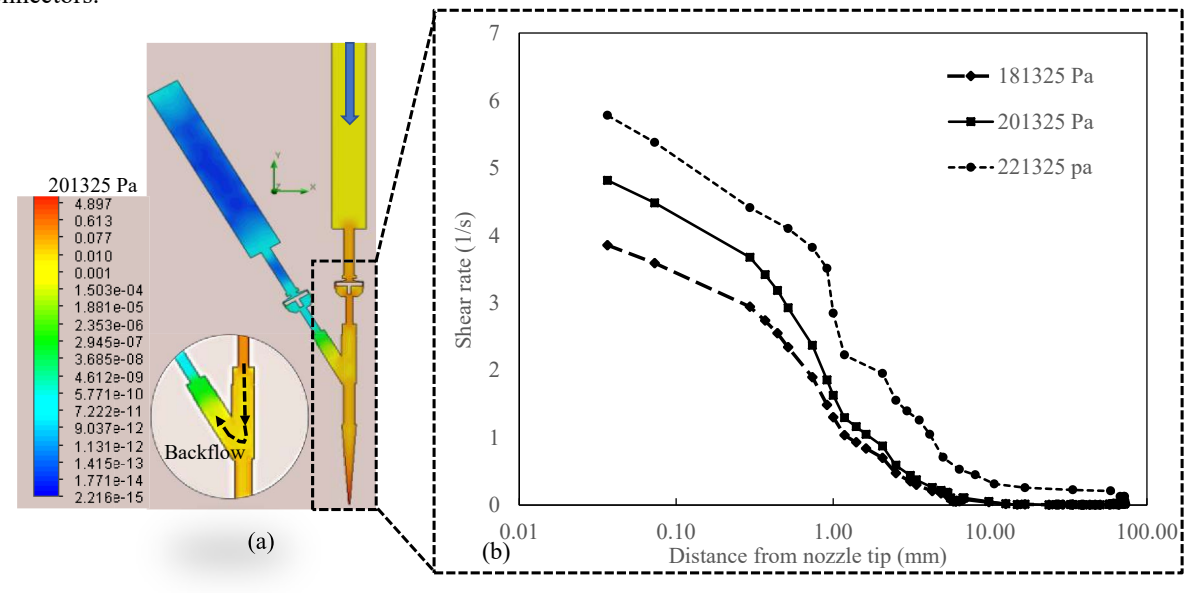


Figure 2: (a) Distribution of shear rate in 30⁰ nozzle connectors for 201325 Pa applied pressure and (b) Distribution of shear rate for three applied pressures of 181325, 201325, and 221325 Pa from nozzle tip to 73.47 mm.

3.2 Fabricated metal nozzle connectors and materials flow through them

Following the methods described in section 2.3, we fabricated total three nozzle connectors having 30°, 45°, and 90° angles as shown in Figure 3 (a-i), (b-i), and (c-i). As illustrated in Figures 3 (a-iii), (b-iii), and (c-iii), all connectors

were used to calculate the time it took for one material (M_1) to transition into another (M_2) . Up until it reached the tip, material from one nozzle was fully extruded into the vacant nozzle connector. Axial delay time is the amount of time needed for this procedure. The substance from the other nozzle was constantly extruded until it was clearly visible at the nozzle tip. "Tilted delay" time is the amount of time required for this procedure. The word "total time" refers to the total of the "axial delay" and the "tilted delay". While 90° had the lowest axial time, the nozzle connector with 30° displayed the highest. One possible reason is the intersection length of the axial and tilted connectors of the nozzles with 30° and 45° correspondingly is 100% and 41% longer than that of the nozzle with 90° , as shown in Figures 3 (a-ii), (b-ii), and (c-ii). Higher intersection length may allow material entry to tilted connection even if we employed check valve to prevent material backflow during extrusion through axial connector. The nozzles with 45° and 90° exhibited the lowest titled delay time in the case of the tilted connector compared to 30° . For both 45° and 90° , material M_1 entered the tilted nozzle with little force during axial flow, causing material M_2 to flow quicker. As illustrated in Figure 3(d), the nozzle connector with angles 45° and 90° had the shortest overall time to switch from material M_1 to material M_2 .

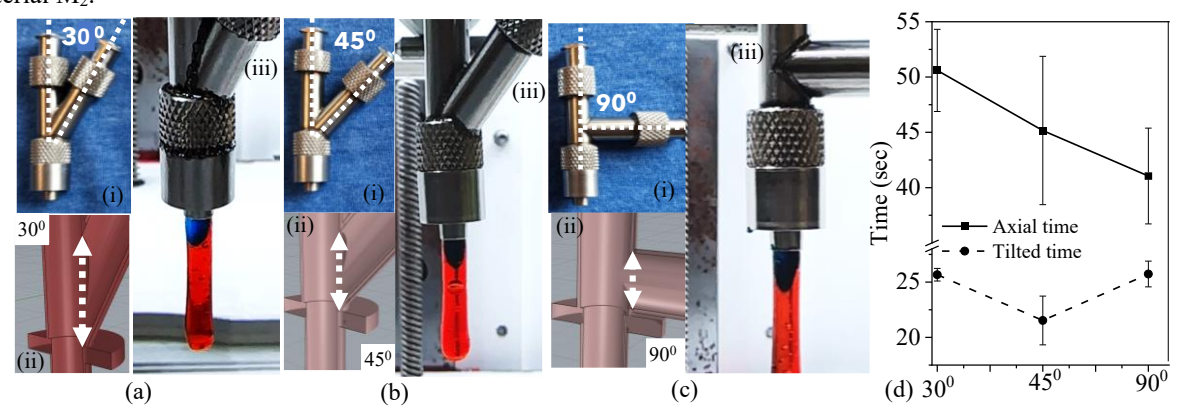


Figure 3: (a) (i) Fabricated nozzle connector with 30^0 angle, (ii) Intersection length for nozzle connector with 30^0 angle, (iii) Transition from material M_1 to material M_2 ; (b) (i) Fabricated nozzle connector with 45^0 angle, (ii) Intersection length for nozzle connector with 45^0 angle, (iii) Transition from material M_1 to material M_2 ; (c) (i) Fabricated nozzle connector with 90^0 angle, (ii) Intersection length for nozzle connector with 90^0 angle, (iii) Transition from material M_1 to material M_2 , (d) Transition time for axial and tilted positions.

3.3 Material distribution through metallic nozzle connectors

To demonstrate the material transition and distribution into filament, we used 45° nozzle connector. A set of filaments were fabricated and the material distribution throughout the filament was examined as shown in Figure 4. The manufactured filament was cut to get cross sections at various filament positions. Those cross sections were crosslinked with CaCl₂ for 5-7 minutes to examine the material distribution, as shown in Figure 4 (b). Even though the manufactured filament had a nearly circular shape after crosslinking, it lost that shape during slicing. From the cross-sectional view of the filament (Figure 4(b)), we observed that filament extruded through the nozzle connectors having angle 45° showed smooth material transition. The photos of the cross sections were processed using Rhino and ImageJ tools to examine the material distribution. The material distribution is shown in Figure 4(d) where at the locations 1, 2 and 3, we observed 68, 56, and 20% M₁. The material distribution through 410 μm is also shown in Figure 4(e).

3.4 Scaffolds fabricated through needle connected to the metallic nozzle connector.

Finally, we created scaffolds with nozzle connectors angled at 45° . A_4C_4 was made and either red (M_1) or blue (M_2) food coloring was used to dye the two syringes. Both syringes had check valves placed between the nozzle and syringes, and they were then loaded onto the printer. First, a layer of material in the color red was extruded, then one in the color blue. The material moving from red to blue was clear from Figure 5(a) to Figure 5(f) of the flow diagram.

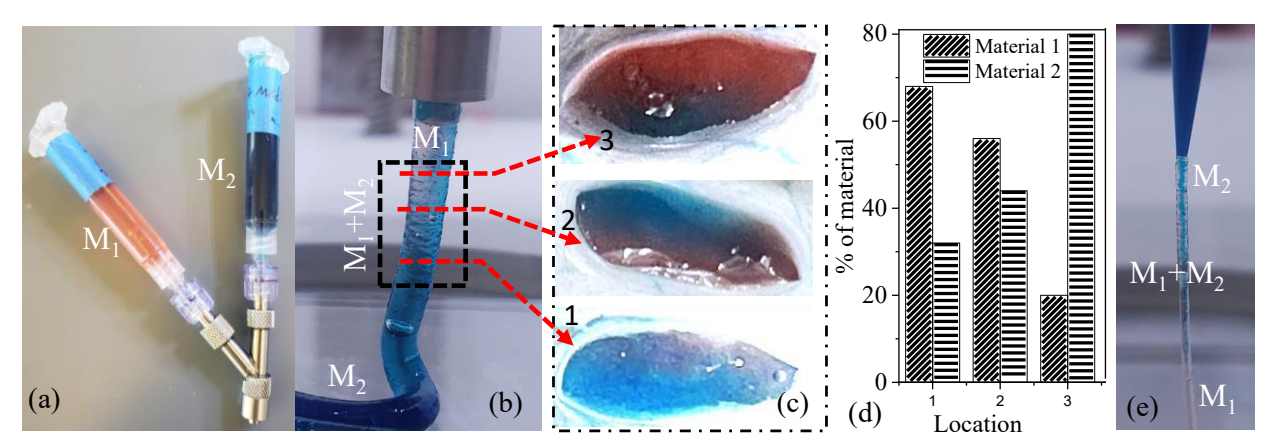


Figure 4: (a) Loading material M_1 and M_2 into two syringes for a 45^0 nozzle connector, (b) Extruding materials through the nozzle connector, (c) Distribution of material M_1 and M_2 at locations 1, 2, and 3 for 45^0 nozzle connector, (d) Percentage of material distribution at locations 1, 2, and 3 for 45^0 nozzle connector, and (e) The material distribution through $410 \ \mu m$ nozzle.

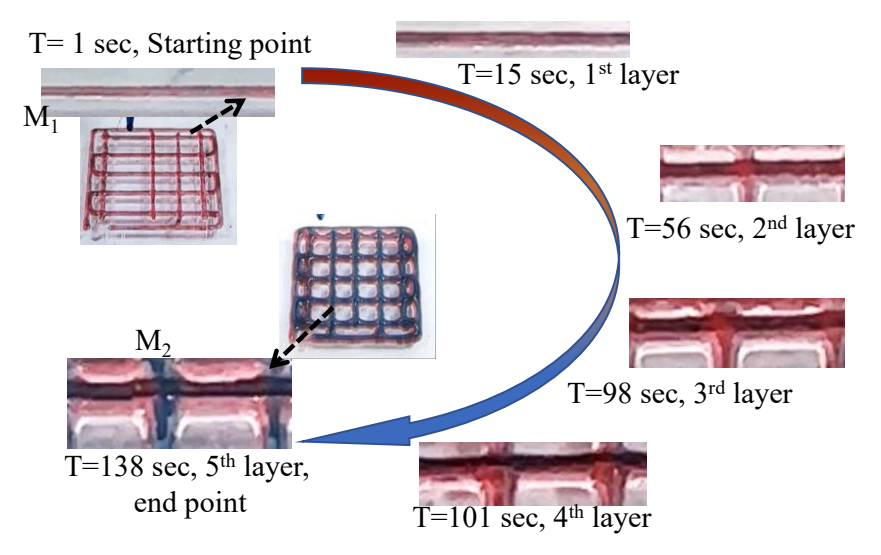


Figure 5: Material distribution throughout the printing process from material 1 to material 2.

4. Conclusion

This work demonstrates the extension of our previous work where we considered angles of 30°, 45°, and 90° (vertical and slanted) between the two materials and decided to construct nozzle connectors out of stainless steel. To examine the effects of 45° angle, we calculated and contrasted the total switching time of the material. A test substance was employed to see how well our previously created hybrid hydrogel (4% Alginate and 4% Carboxymethyl Cellulose, CMC) flowed through the nozzle system. Through the nozzle connector and nozzle, itself, we carefully studied the material distribution into the filament during the extrusion process. Identifying the material transition time during extrusion through the nozzle and connecting it to all nozzle connectors will be done going forward. We will also determine how material viscosity affects the material transition for all connectors and nozzles attached to the connector (with material compositions other than A₄C₄). Our future includes implementing a start-stop method to print materials M1 and M2 separately, without any blending between them. Finally, our long-term objective is to extrude various materials containing living cells using those nozzle connectors.

Acknowledgements

Research was supported by New Hampshire-EPSCoR through BioMade Award #1757371 from National Science Foundation and New Hampshire-INBRE through an Institutional Development Award (IDeA), P20GM103506, from the National Institute of General Medical Sciences of the NIH.

References

- [1] S. Kyle, Z. M. Jessop, A. Al-Sabah, and I. S. Whitaker, "'Printability'of Candidate Biomaterials for Extrusion Based 3D Printing: State-of-the-Art," *Advanced healthcare materials*, vol. 6, no. 16, p. 1700264, 2017.
- [2] S. V. Murphy and A. Atala, "3D bioprinting of tissues and organs," *Nature biotechnology*, vol. 32, no. 8, pp. 773-785, 2014.
- [3] H.-J. Kong, K. Y. Lee, and D. J. Mooney, "Decoupling the dependence of rheological/mechanical properties of hydrogels from solids concentration," *Polymer*, vol. 43, no. 23, pp. 6239-6246, 2002.
- [4] J. Malda *et al.*, "25th anniversary article: engineering hydrogels for biofabrication," *Advanced materials*, vol. 25, no. 36, pp. 5011-5028, 2013.
- [5] C. Mandrycky, Z. Wang, K. Kim, and D.-H. Kim, "3D bioprinting for engineering complex tissues," *Biotechnology Advances*, vol. 34, no. 4, pp. 422-434, 2016/07/01/ 2016, doi: https://doi.org/10.1016/j.biotechadv.2015.12.011.
- [6] P. Lewis and R. N. Shah, "3D-Printed gelatin scaffolds of differing pore size and geometry modulate hepatocyte function and gene hxpression," (in English), *Frontiers in Bioengineering and Biotechnology*, Abstract, doi: 10.3389/conf.FBIOE.2016.01.01756.
- [7] D. B. Kolesky, K. A. Homan, M. A. Skylar-Scott, and J. A. Lewis, "Three-dimensional bioprinting of thick vascularized tissues," *Proceedings of the National Academy of Sciences*, vol. 113, no. 12, pp. 3179-3184, 2016.
- [8] J.-H. Shim, J.-S. Lee, J. Y. Kim, and D.-W. Cho, "Bioprinting of a mechanically enhanced three-dimensional dual cell-laden construct for osteochondral tissue engineering using a multi-head tissue/organ building system," *Journal of Micromechanics and Microengineering*, vol. 22, no. 8, p. 085014, 2012.
- [9] T. Xu *et al.*, "Hybrid printing of mechanically and biologically improved constructs for cartilage tissue engineering applications," *Biofabrication*, vol. 5, no. 1, p. 015001, 2012.
- [10] K. Hixon, C. Eberlin, P. Kadakia, S. McBride-Gagyi, E. Jain, and S. Sell, "A comparison of cryogel scaffolds to identify an appropriate structure for promoting bone regeneration," *Biomedical Physics & Engineering Express*, vol. 2, no. 3, p. 035014, 2016.
- [11] T. K. Merceron *et al.*, "A 3D bioprinted complex structure for engineering the muscle-tendon unit," *Biofabrication*, vol. 7, no. 3, p. 035003, 2015.
- [12] J. Kundu, J. H. Shim, J. Jang, S. W. Kim, and D. W. Cho, "An additive manufacturing-based PCL-alginate-chondrocyte bioprinted scaffold for cartilage tissue engineering," *Journal of tissue engineering and regenerative medicine*, vol. 9, no. 11, pp. 1286-1297, 2015.
- [13] S. Sakai, K. Ueda, E. Gantumur, M. Taya, and M. Nakamura, "Drop-On-Drop Multimaterial 3D Bioprinting Realized by Peroxidase-Mediated Cross-Linking," *Macromolecular rapid communications*, vol. 39, no. 3, p. 1700534, 2018.
- [14] L. Ruiz-Cantu, A. Gleadall, C. Faris, J. Segal, K. Shakesheff, and J. Yang, "Multi-material 3D bioprinting of porous constructs for cartilage regeneration," *Materials Science and Engineering: C*, vol. 109, p. 110578, 2020.
- [15] C. Nelson, S. Tuladhar, and M. A. Habib, "Designing an Interchangeable Multi-Material Nozzle System for 3D Bioprinting Process," in *International Manufacturing Science and Engineering Conference*, 2021, vol. 85062: American Society of Mechanical Engineers, p. V001T03A005.
- [16] A. Habib, V. Sathish, S. Mallik, and B. Khoda, "3D printability of alginate-carboxymethyl cellulose hydrogel," *Materials*, vol. 11, no. 3, p. 454, 2018.
- [17] A. Habib and B. Khoda, "Effect of Process parameters on cellulose fiber alignment in bio-printing," ed: MSEC, ASME, 2019.